frontiers in Energy Research

ORIGINAL RESEARCH
published: 30 July 2021
doi: 10.3389/fenrg.2021.702952

Feasibility Study for the Fast Periodic Pulsed Reactor with UO_2 Fuel

Liang Zhang[1†], *Xinbiao Jiang*[1*†], *Xinyi Zhang*[1,2†], *Tengyue Ma*[1,2], *Sen Chen*[1], *Lipeng Wang*[1], *Da Li*[1] *and Lixin Chen*[1]

[1]State Key Laboratory of Intense Pulsed Radiation Simulation and Effect (Northwest Institute of Nuclear Technology), Xi'an, China, [2]Xi'an High Technology Institute, Xi'an, China

In order to study the feasibility of the fast periodic pulsed reactor with UO_2 as fuel (abbreviated as FPPRU), the core models with different load schemes are designed. Neutronic characteristics of two typical design schemes are compared, and the better design scheme is determined. The critical search method is established for analyzing the reactor dynamics. Furthermore, the theoretical estimation formulas are derived to study the factors affecting the reactor dynamics clearly and intuitively. The reactor dynamics of the fast periodic pulsed reactor with UO_2 and PuO_2 as fuel are compared. The thermal hydraulic characteristic of FPPRU is studied with the sub-channel model. The results show that the design scheme of the FPPRU meets the demand of neutronics and thermal hydraulics safety. Meanwhile, the pulse parameter quality of the FPPRU with UO_2 as fuel is not as good as that of IBR-2 with PuO_2 as fuel.

Keywords: pulse parameters, periodic, pulsed reactor, UO_2, feasibility

OPEN ACCESS

Edited by:
Qian Zhang,
Harbin Engineering University, China

Reviewed by:
Peiwei Sun,
Xi'an Jiaotong University, China
Quan Gan,
Hefei Institutes of Physical Science (CAS), China
Jinsen Xie,
University of South China, China

****Correspondence:***
Xinbiao Jiang
zhangliang9@nint.ac.cn

†These authors have contributed equally to this work and share first authorship

Specialty section:
This article was submitted to Nuclear Energy, a section of the journal Frontiers in Energy Research

Received: *30 April 2021*
Accepted: *25 June 2021*
Published: *30 July 2021*

Citation:
Zhang L, Jiang X, Zhang X, Ma T, Chen S, Wang L, Li D and Chen L (2021) Feasibility Study for the Fast Periodic Pulsed Reactor with UO_2 Fuel. Front. Energy Res. 9:702952. doi: 10.3389/fenrg.2021.702952

INTRODUCTION

The fast periodic pulsed reactor uses rotating reflectors to introduce periodic reactivity, making the core generate power pulses at a certain frequency. The fast periodic pulsed reactor IBR-2 had been built in 1984 in the Joint Institute for Nuclear Research of Russia and had retired in 2006. And then the modernized reactor IBR-2M was designed and built and was put into use in 2011 (Dragunov et al., 2012). After successful operation for as long as 37 years, the fast periodic pulsed reactor IBR-2/IBR-2M has been proven to be safe. IBR-2/IBR-2M could provide pulsed neutron flux with narrow half-width and high intensity. Lots of research has been carried out in a wide range of scientific fields, including condensed physics, biology, chemistry, material, geophysics, new superconductivity, and heavy metal nuclear database (Marina, 2011; Ata-Allah et al., 2016; Avdeev et al., 2019; Badawy et al., 2020; Golovin et al., 2020; Turchenko et al., 2020).

So far, lots of studies are performed on many aspects of IBR-2/IBR-2M, such as operation lifetime, neutron flux, reactor dynamics, and reactor safety. For example, in order to increase the operation lifetime of IBR-2M, in 2020, Ananiev studied the way to optimize the reactor fuel run by reshuffling fuel assemblies, giving more uniform fuel burn up and increasing the core lifetime by almost 1/4 (Ananiev et al., 2020). For improving the neutron flux, in 2018, Ananiev considered the neutronic aspect of the IBR-2 reactor optimization and studied the way to increase the thermal neutron flux theoretically (Ananiev et al., 2019). In 2013, Kulikov studied the way to optimize the cold-neutron yield and found the best material for use in IBR-2M cold moderators (Kulikov and Shabalin, 2013). The reactor dynamics plays a very important role in the operation and safety of this kind of reactor. In 2017, Pepelyshev analyzed the transient processes caused by intentional periodic oscillations of the reactivity and investigated the fast feedback parameters of IBR-2M (Pepelyshev et al., 2017). In 2015, Pepelyshev simulated the transitional processes at a wide range of reactivity change and power

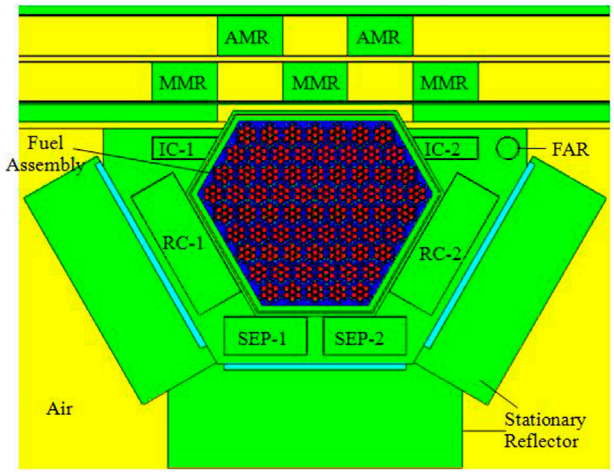

FIGURE 1 | IBR-2M core.

change, and the result is in good accordance with the detected one (Pepelyshev et al., 2015). In 2010, Chan and Pepelyshev studied the IBR-2 dynamics with power shedding (Chan and Pepelyshev, 2010). In 2008, Chan and Pepelyshev studied the power feedback dynamics taking account of slow components (Chan and Pepelyshev, 2008). In 2006, Pepelyshev analyzed the power pulse shape measured over the entire dynamic range of neutron flux variation and found out how to obtain best approximation to the experimental data (Pepelyshev and Popov, 2006a). And Pepelyshev successfully used the dynamical method to determine the reactivity effects of two types of moving reflectors in the pulsed regime of IBR-2 reactor operating at power (Pepelyshev and Popov, 2006b). For the modernization from IBR-2 to IBR-2M, Dragunov

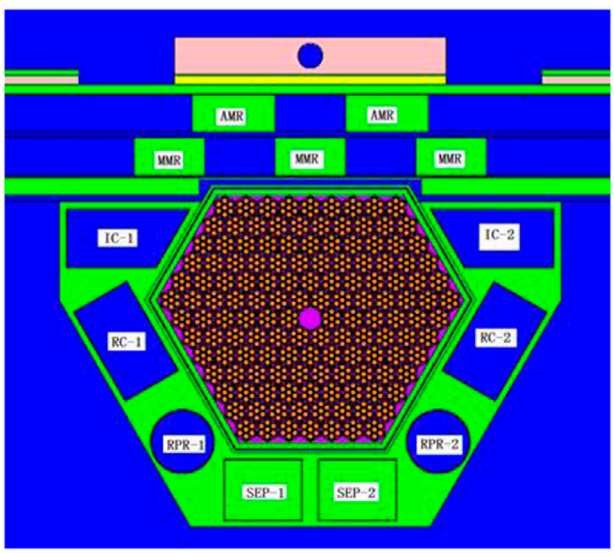

FIGURE 2 | Design scheme of FPPRU1.

introduced the project modernizing the reactor and the technical characteristics before and after modernization (Dragunov et al., 2012). For the safety of IBR-2, in 2010, Pepelyshev discussed the safety and reliability of the reactor and showed how a series of safety problems related to IBR-2 reactor physics are resolved (Pepelyshev et al., 2010).

Till now, almost all the research studies aimed at the IBR-2 type reactor with PuO_2 as fuel. As UO_2 fuel is very widely used in nuclear reactors, the use of UO_2 may promote the development of the fast periodic pulsed reactor. The study on the feasibility of such reactor using UO_2 fuel is very meaningful. The fast periodic pulsed reactor with UO_2 fuel (abbreviated as FPPRU) is designed in this article. And the feasibility is studied from the view of neutronics, dynamics, thermal hydraulics, and so on.

METHODS AND RESULTS

Conceptual Design of the FPPRU

Brief Description of IBR-2M

As the conceptual design of the fast periodic pulsed reactor with UO_2 as fuel is on the basis of IBR-2M, the structure of IBR-2M is briefly introduced here. As shown in **Figure 1**, the IBR-2M core is of an irregular hexagonal shape consisting of 69 PuO_2 fuel assemblies and is cooled by liquid sodium. Outside the core, there are two kinds of reflectors. One is the stationary reflector and the other is the moving reflector, which consists of one main moving reflector (MMR in **Figure 1**) and one auxiliary moving reflector (AMR in **Figure 1**). Seven control rods are used to regulate the reactivity, including two regulating rods (IC-1 and IC-2 in **Figure 1**), two compensating rods (RC-1 and RC-2 in **Figure 1**), two safety rods (SEP-1 and SEP-2 in **Figure 1**), and one fine adjusting rod (FAR in **Figure 1**). The material of all the reflectors and control rods is stainless steel. MMR and AMR are located on one side, opposite the core. The unique feature of the reactor is that it controls the periodic change of reactivity through the movable reflectors MMR and AMR outside the reactor and generates continuous pulses at a certain frequency. The rotating speeds of MMR and AMR are 600r/min and 300r/min, respectively, and the rotating directions are opposite. At a period of 200 ms, the two reflectors pass simultaneously opposite the core. At the very moment, the combination of the two reflectors could cover the neutron flight direction toward the core's periphery, and the core changes from deep subcritical state to transient supercritical state, generating continuous power pulses at a frequency of 5 Hz. The average thermal power and peak pulse power are 2 and 1500 MW, respectively.

Design Schemes of the FPPRU

In this article, different conceptual design schemes for the fast periodic pulsed reactor with UO_2 as fuel (FPPRU) are made. And two schemes are analyzed in detail. One is named as FPPRU1, whose reflectors and control rods are made of stainless steel, the same as IBR-2M. The other is named as FPPRU2, whose reflectors use beryllium, which could effectively reduce the number of UO_2 fuel assemblies. The material of FPPRU2

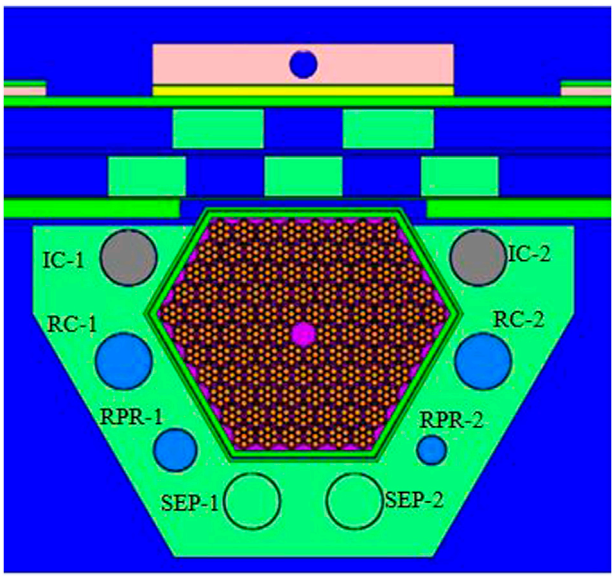

FIGURE 3 | Design scheme of FPPRU2.

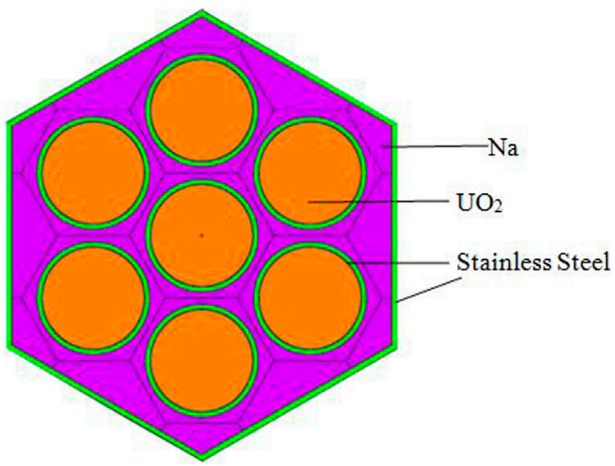

FIGURE 4 | Structure of the fuel assembly of FPPRU1 and FPPRU2.

control rods is B_4C. FPPRU1 and FPPRU2 are shown in **Figures 2**, **3**, respectively. In **Figure 2** and **Figure 3**, from the left to the right is the direction of the X-axis, and from the bottom to the top is the direction of the Y-axis. The coordinate of the center of the core on the X-axis is 0. The structure of the fuel assembly of FPPRU1 and FPPRU2 is the same, as shown in **Figure 4**. It could be seen that, compared to IBR-2M, more UO_2 fuel assemblies are needed to reach criticality for FPPRU. The main reason is that the critical mass of U-235 reactor is greater than that of Pu-239 reactor.

FPPRU1 consists of 139 hexagonal assemblies, including 138 UO_2 fuel assemblies and one neutron source assembly located in the center of the core, as shown in **Figure 2**. The reflector of FPPRU1 contains the stationary reflector and the moving reflector. Inside the stationary reflector there are eight control rods for regulating the reactivity, including two regulating rods (IC-1 and IC-2 in **Figure 2**), two cubic compensating rods (RC-1 and RC-2 in **Figure 2**), two cylindrical compensating rods (RPR-1 and RPR-2 in **Figure 2**), and two safety rods (SEP-1 and SEP-2 in **Figure 2**). The moving reflector consists of one main moving reflector MMR and one auxiliary moving reflector AMR, which are both arranged opposite one side of the core, as shown in **Figure 2**. The material of both reflectors and control rods is stainless steel. The periodic reactivity is accomplished by the combination of the moving reflector MMR and auxiliary moving reflector AMR (MMR and AMR in **Figure 2**). The rotation speeds of MMR and AMR are 600 r/min and 300 r/min, respectively. For each period (T = 200 ms), when AMR and MMR arrive at the position in **Figure 2**, the two reflectors completely block the leakage path of neutrons outward, and the reactivity reaches the maximum. After AMR and MMR move away from the position in **Figure 2**, the reactivity gradually decreases and finally stabilizes to the minimum ρ_b, forming the change of reactivity and power shown in **Figure 5**.

As shown in **Figure 5**, under the stable operation of the fast periodic pulsed reactor, the reactivity $\rho(t)$ and power $P(t)$ vary periodically at a certain frequency. T is the period, and each period could be divided into two phases: pulse phase and background phase. For the first period from time 0~T, OAB (from time 0~t_b) stands for the pulse phase and BC (from time t_b~T) stands for the background phase. t_h is the half-width of the pulse. ρ_{max} is the maximum reactivity, and ρ_b is the background reactivity. P_{max} is the maximum power, and P_b is the background power. There is little change in the reactivity within BC, and ρ_b could be approximated as a constant. In one period, the integral of power from 0~T and from t_b ~T are the total energy E_t and the background energy E_b, respectively. The integral of power from 0 ~ t_b is the pulse energy E_p, and $E_p = E_t - E_b$.

FPPRU2 consists of 101 hexagonal assemblies, including 100 UO_2 fuel assemblies and one neutron source assembly located in the center of the core. All the assemblies are arranged in a double-layer stainless steel barrel. The reflector of FPPRU contains the stationary reflector and the moving reflector. Inside the stationary reflector, there are eight control rods for regulating the reactivity, including two regulating rods (IC-1 and IC-2 in **Figure 3**), four compensating rods (RC-1, RC-2, RPR-1, and RPR-2 in **Figure 3**), and two safety rods (SEP-1 and SEP-2 in **Figure 3**). The moving reflector consists of one main moving reflector MMR and one auxiliary moving reflector AMR (MMR and AMR in **Figure 3**), which are both arranged opposite to one side of the core, as shown in **Figure 3**. FPPRU2 produces power pulses in the same way with FPPRU1. Different from FPPRU1, the materials of the reflectors and control rods of FPPRU2 are beryllium and B_4C, respectively.

As shown in **Figure 4**, each fuel assembly consists of seven fuel elements and 0.5 mm thick outer stainless steel cladding. The outer radius of the fuel assembly is 3.464 cm. The distance between adjacent fuel elements in the assembly is 1.11 cm. Each fuel element is made up of UO_2, He gas gap, and

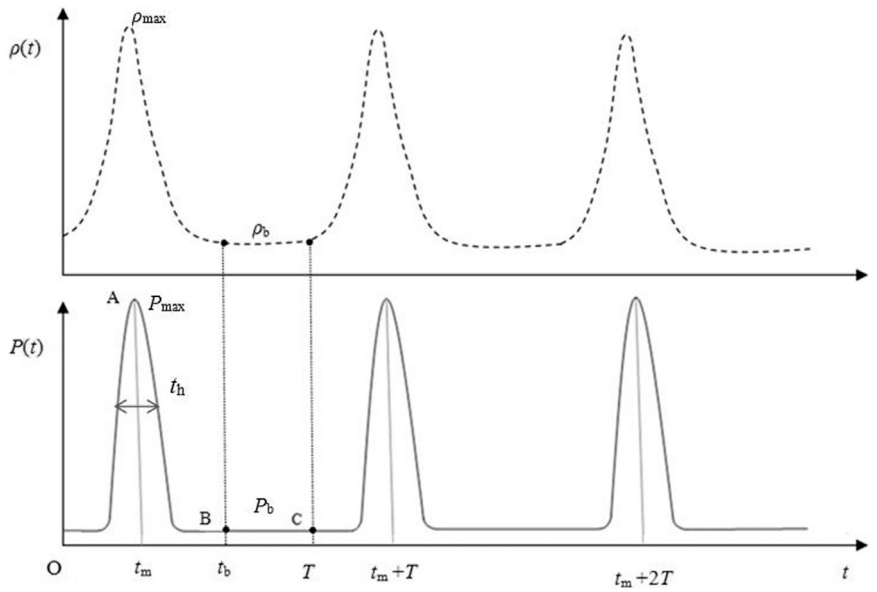

FIGURE 5 | Power and reactivity change of the fast periodic pulsed reactor.

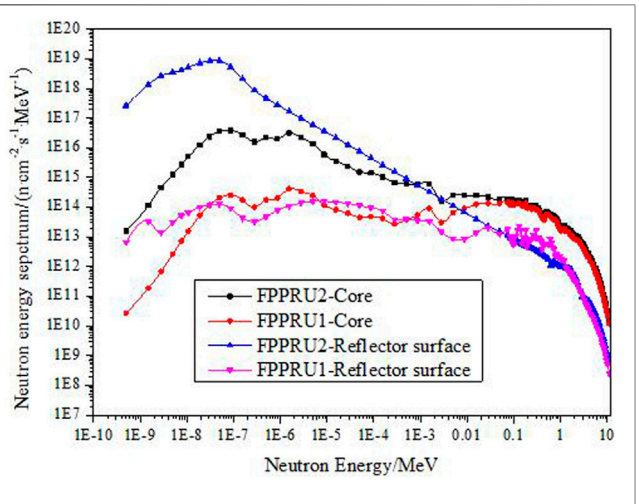

FIGURE 6 | Maximum effective multiplication factor k_{eff} vs. the enrichment of U-235.

stainless steel cladding from inside to outside, and the outer radius are 0.45, 0.46, and 0.50 cm, respectively. The length of the UO_2 active zone of the fuel element is 50 cm. Up and down the active zone are both the axial reflectors with 10 cm length. The materials of the axial reflectors of FPPRU1 and FPPRU2 are stainless steel and beryllium, respectively.

Calculation of Neutronic Parameters and Determination of Core Design Schemes

The neutronic parameters of FPPRU1 and FPPRU2, including the criticality, dynamic parameters, neutron energy spectrum, and power distribution, are calculated in the paper using the MCNP code. And based on the neutronic characteristics, the core design scheme is determined.

Criticality

In the design of the FPPRU, considering the burn up during the reactor lifetime, the uncertainty of U-235 enrichment, and the impurity of the reactor reflector, the reserved reactivity ρ_r should not be less than about 45 mk (1mk = 0.001), ensuring the long-term operation for the reactor. **Figure 6** shows the relationship between the maximum effective multiplication factor k_{eff} vs. the enrichment of U-235 for several core design schemes.

As shown in **Figure 6**, for FPPRU1, when U-235 enrichment is 75%, the reserved reactivity ρ_r ($\rho_r = (k_{eff}-1)/k_{eff}$) is 47.69 mk. For FPPRU2, when U-235 enrichment is 77%, the reserved reactivity ρ_r is 44.87 mk. These two core loading schemes basically meet the requirement of reserved reactivity and can reach a shutdown margin over −25 mk (−28.63 mk and −27.05 mk for FPPRU1 and FPPRU2, respectively).

The maximum effective multiplication factor k_{eff} of IBR-69UO_2 is also given in **Figure 6**. IBR-69UO_2 is the reactor that only replaces the PuO_2 fuel of the IBR-2M reactor with the UO_2 fuel. The k_{eff} of IBR-69UO_2 clearly shows that more fuel assemblies must be used to reach criticality if UO_2 is used as fuel.

Dynamic Parameters

The effective delayed neutron fraction β_{eff} and neutron generation time Λ play very important roles in reactor dynamics. For the fast periodic pulsed reactor, these two dynamic parameters have great influence on the dynamics under periodic pulse operation. β_{eff} and Λ are calculated for several reactors with different reflector materials using the MCNP code, as shown in **Table 1**.

TABLE 1 | Calculating results of the effective delayed neutron fraction β_{eff} and neutron generation time Λ.

Reactor	Fuel	Fuel assembly number	Reflector material	Λ/ns	$\beta_{eff}/10^{-5}$
IBR-2M	95% PuO_2	69	Stainless steel	65 Pepelyshev and Popov (2006a)	216 Pepelyshev and Popov (2006a)
			Beryllium	327	203
FPPRU1	75% UO_2	138	Stainless steel	114.9	728
FPPRU2	77% UO_2	100	Beryllium	1,477	736

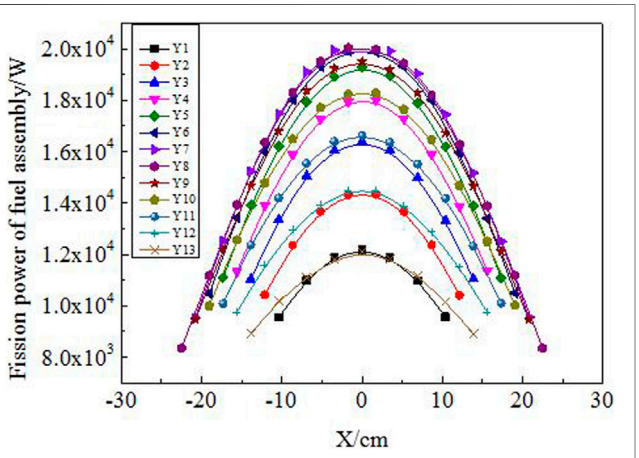

FIGURE 7 | Neutron energy spectrum.

The IBR-2M reactor uses PuO_2 as fuel, and the reflector is made of stainless steel. The neutron generation time is 65 ns, and the half-width of the pulse is 245 μs (Pepelyshev and Popov, 2006a). In general, the smaller the neutron generation time, the narrower the half-width of the pulse. Since the design is intended to achieve a narrower half-width, it is hoped that the neutron generation time could be as small as possible. As could be seen from **Table 1**, if the material of the IBR-2M reflector is replaced with beryllium, the neutron generation time Λ will increase significantly to 327 ns. Compared with stainless steel, beryllium is a much better material for slowing down neutrons. More fast neutrons will be moderated to thermal neutrons in the reflector and would be reflected back to the core, which will both make the neutrons disappear much slower and increase the neutron generation time Λ significantly. For the same reason, the FPPRU2 reactor using beryllium as the reflector material requires fewer fuel assemblies to reach criticality than FPPRU1 using stainless steel as the reflector material. The neutron generation time Λ of FPPRU2 is as high as 1,477 ns, much higher than 114.9 ns of FPPRU2. Therefore, from the view of the half-width of the pulse, FPPRU1 with a stainless steel reflector would be better. It can also be seen from **Table 1** that the effective delayed neutron fraction β_{eff} of FPPRU1 and FPPRU2 with UO_2 as fuel are similar, and are both much higher than that of IBR-2M with PuO_2 as fuel. It is mainly due to that more delayed neutrons are released in the fission of U-235. In addition, the difference between energy spectrums of IBR-2 and FPPRU also has some influence.

Neutron Energy Spectrum

Figure 7 shows the neutron energy spectrum in the core and on the stationary reflector surface of FPPRU1 and FPPRU2 at average power 2 MW. **Table 2** shows the neutron flux density and the average neutron energy in the core and on the stationary reflector surface. The neutrons are divided into four groups by energy, that is, the thermal group (0–0.414 eV), the epithermal group (0.414 eV–10 keV), the fast group one (0.01–0.1 MeV), and the fast group two (0.1–10 MeV). The mean neutron energy in the cores of FPPRU1 and FPPRU2 are 0.9243 and 0.9186 MeV, respectively. The average neutron energy on the stationary reflector surface of FPPRU1 and FPPRU2 are 0.5505 and 0.3596 MeV, respectively. The neutron energy spectrum on the surface of FPPRU2 reflector is softer than that on the surface of FPPRU1. It means that FPPRU2 is inferior to obtain a faster neutron beam. The main reason is that much more neutrons are moderated by beryllium in FPPRU2. As faster neutron beam is expected to be achieved in the design, from the view of the neutron energy spectrum, the FPPRU1 core scheme is preferred in this article. In addition, the fast neutron flux density (>0.01 MeV) in the core and on the stationary reflector surface of FPPRU1 are 8.88×10^{13} n/(cm^2·s) and 8.10×10^{12} n/(cm^2·s), respectively.

Power Distribution

The fission power distribution of FPPRU1 and FPPRU2 fuel assemblies at average power 2 MW is shown in **Figures 8**, **9**, respectively. From the bottom to the top of FPPRU1 core (**Figure 2**), Y1,Y2, . . ., Y13 in **Figure 8** stand for the first layer, second layer, . . . thirteenth layer fuel assemblies, respectively. And from the bottom to the top of FPPRU2 core (**Figure 3**), Y1,Y2, . . ., Y11 in **Figure 9** stand for the first layer, second layer, . . . eleventh layer fuel assemblies, respectively. X in **Figures 8**, **9** represents the coordinate of each fuel assembly in the direction of the X axis, and the coordinate of the center of the core on the X axis is 0.

From **Figures 8**, **9** it could be seen that the closer the fuel assembly to the center of FPPRU1 core, the greater the fission power basically. However, for FPPRU2, the fission power of Y1 layer fuel assemblies is the largest. As the safety rods of FRRPU2 (SEP-1 and SEP-2 in **Figure 3**) are at the top in the calculation, downside the Y1 layer fuel assemblies are all beryllium reflector. Beryllium moderates neutrons and reflects neutrons back to the core. The thermal neutrons are much more in the Y1 layer fuel assemblies, and thus, the fission power is higher than that of other layer fuel assemblies. It could also be seen from **Figure 9** that the fission power of FPPRU2

TABLE 2 | Neutron flux density and average neutron energy for FPPRU1 and FPPRU2.

Reactor	Counting range	Neutron flux density/(n·cm^{-2}·s^{-1})				Average energy/MeV
		0–0.414 eV	0.414 eV–10 keV	0.01–0.1 MeV	0.1–10 MeV	
FPPRU1	Core	5.7608×10^{7}	6.6636×10^{11}	1.1875×10^{13}	7.6966×10^{13}	0.9243
	Stationary reflector surface	6.4718×10^{7}	1.5492×10^{11}	1.2734×10^{12}	6.8292×10^{12}	0.5505
FPPRU2	Core	9.1157×10^{9}	3.5443×10^{12}	1.7740×10^{13}	9.8845×10^{13}	0.9186
	Stationary reflector surface	1.0545×10^{12}	4.0293×10^{12}	1.5076×10^{12}	3.3023×10^{12}	0.3596

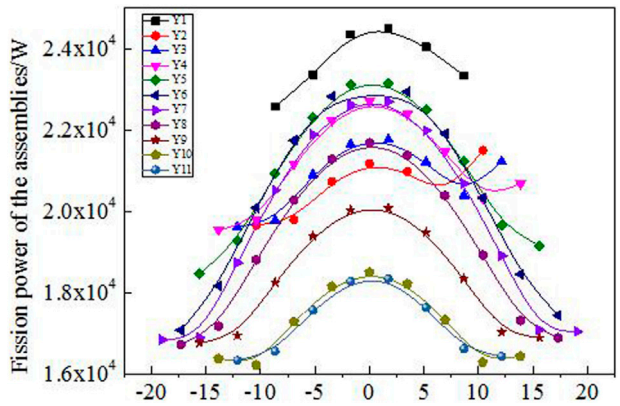

FIGURE 8 | Fission power distribution of FPPRU1.

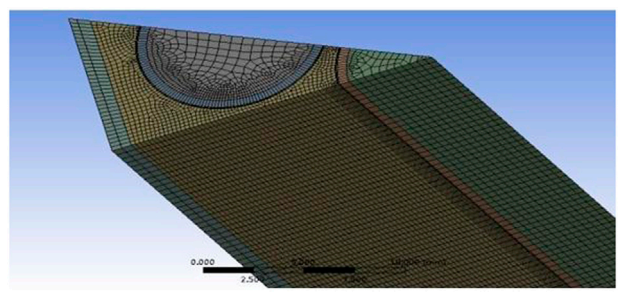

FIGURE 9 | Fission power distribution of FPPRU2.

Y1,Y2,Y3, and Y4 layers is not symmetric. The reason is that the size of the two compensating rods RPR-1 and RPR-2 in **Figure 3** is not the same in the design.

The fission energy deposition and gamma energy deposition in the core components, including the auxiliary moving reflector, the control rod, and the fuel assembly, are shown in **Table 3**. According to **Table 3**, at average power 2 MW, the maximum energy deposition in the fuel assembly of FPPRU1 and FPPRU2 is 19.65 and 22.86 kW, respectively. The nonuniformity coefficient of FPPRU1 radial power is 1.383, which is larger than 1.225 of FPPRU2. The reason is that FPPRU2 reflector (beryllium) could moderate neutrons much better and the power of the outer fuel assemblies is relatively higher.

The energy deposition in the stationary beryllium reflector of FPPRU2 is 12 kW, which is 3.72 times as much as that in the stationary stainless steel reflector of FPPRU1. The material of FPPRU1 and FPPRU2 control rods is stainless steel and B_4C, respectively. Among the eight control rods of FPPRU2, the compensating rod (RC-1 or RC-2 in **Figure 3**) has the largest energy deposition 2.48 kW. For FPPRU1, the compensating rod (RC-1 or RC-2 in **Figure 2**) also has the largest energy deposition, and the value is 0.71 kW. Therefore, under the condition of natural air cooling, the thermal safety of the stationary reflector of FPPRU1 is better.

Determination of Core Design Schemes

Compared with the FPPRU1 design scheme, the advantages of FPPRU2 design scheme are that less fuel assemblies are needed to reach criticality, and the nonuniformity coefficient of the radial power is smaller. However, the disadvantages of FPPRU2 are more obvious. The neutron generation time of FPPRU2 is too long to achieve ideal neutron pulse with narrow half-width. The neutron energy spectrum of FPPRU2 is softer, not beneficial for producing more fast neutrons. The energy deposition in the stationary reflector is much more, not conductive to heat dissipation. As the purpose of the design is to achieve narrower half-width pulse and harder neutron energy

TABLE 3 | Energy deposition of core components for FPPRU1 and FPPRU2.

Core components	FPPRU1		FPPRU2	
	Fission energy deposition/W	Gamma energy deposition/W	Fission energy deposition/W	Gamma energy deposition/W
Stationary reflector	7.1943×10^{2}	2.5041×10^{3}	8.0620×10^{3}	3.9391×10^{3}
Main moving reflector (MMR)	1.7433×10^{2}	1.4613×10^{3}	1.3332×10^{3}	5.0261×10^{2}
Auxiliary moving reflector (AMR)	1.2036×10^{2}	1.3960×10^{3}	8.9480×10^{2}	4.2971×10^{2}
Control rods (RC-1 or RC-2)	9.5287×10^{1}	6.1124×10^{2}	2.2962×10^{3}	1.8339×10^{2}
Fuel assembly (maximum)	1.8756×10^{4}	9.0146×10^{2}	2.2761×10^{4}	1.0494×10^{3}
Fuel assembly (minimum)	7.8222×10^{3}	3.2879×10^{2}	1.5172×10^{4}	5.9180×10^{2}

spectrum, the design scheme of FPPRU1 is selected. The cost is that more fuel assemblies are needed to reach criticality and the nonuniformity coefficient of the radial power is relatively high.

Reactor Dynamics

Reactor dynamics plays a very important role for the fast periodic pulsed reactor. So far, lots of research have been performed on the dynamics for the IBR-2 type reactor (Pepelyshev and Popov, 2006a; Pepelyshev and Popov, 2006b; Chan and Pepelyshev, 2008; Chan and Pepelyshev, 2010; Pepelyshev et al., 2015; Pepelyshev et al., 2017; Brezhnev et al., 2017). In this article, the critical search method for studying reactor dynamics is established based on the basic characteristics of the fast periodic pulsed reactor. Furthermore, the theoretical estimation formula which could show the difference between FPPRU1 dynamics and IBR-2 dynamics clearly and intuitively is also derived. And the pulse parameters of FPPRU1 and IBR-2 are compared using the critical search method and the theoretical estimation formula.

Critical Search Method

The critical search method is based on the point kinetic model:

$$\frac{\mathrm{d}P(t)}{\mathrm{d}t} = \frac{\rho(t) - \beta_{\mathrm{eff}}}{\Lambda} P(t) + \sum_{i=1}^{6} \lambda_i C_i(t), \tag{1}$$

$$\frac{\mathrm{d}C_i(t)}{\mathrm{d}t} = \frac{\beta_{\mathrm{eff}} \cdot \alpha_i}{\Lambda} P(t) - \lambda_i C_i(t). \tag{2}$$

In **Eqs. 1**, **2**, $\alpha_i = \beta_{\mathrm{eff},i}/\beta_{\mathrm{eff}}$. $\rho(t)$ and $P(t)$ are the reactivity and power in **Figure 5**, respectively. β_{eff} and $\beta_{\mathrm{eff},i}$ are the total and the i^{th}-group effective delayed neutron fraction, respectively. Λ is the neutron generation time and $C_i(t)$ is the density of the i^{th}-group delayed neutron precursor concentration.

From **Eqs. 1**, **2**, $P(t)$ would be obtained if $\rho(t)$ is known. By changing the position of MMR and AMR gradually, the relative change of reactivity $\rho(t)$ could be obtained by calculation or by experiment. Thus, the shape of reactivity $\rho(t)$is known. The shape function is defined as $f(t)$, and then the relationship between $\rho(t)$ and $f(t)$ is as follows:

$$\rho(t) = f(t) + D. \tag{3}$$

In **Eq. 3**, D is a constant. It is known that when the fast periodic pulsed reactor is under the stable operation, the peak power of every period is approximately equal, as shown in **Figure 5**. By gradually changing the value of D and solving **Eqs. 1**, **2** until every peak power is found to approach the same, D could be determined. In the calculation, if the peak power of the 200th period $P_{\max}$ (200) and the peak power of the 500th period $P_{\max}$ (500) could meet the condition $|(P_{\max}(200) - P_{\max}(500))/P_{\max}(500)| < 0.1\%$, then the D value is what we search for.

The dynamic characteristic of the fast periodic pulsed reactor is very special. It is that only one fixed D value exists if the basic parameters of the reactor, including $f(t)$, β_{eff}, Λ, are determined. And with D being one fixed value, the ratio of peak power to average power $P_{\max}/P_{\mathrm{t}}$ and the ratio of background energy to total energy $E_{\mathrm{b}}/E_{\mathrm{t}}$ are also unchangeable. Meanwhile, the absolute power $P_{\max}$ and the absolute energy E_{b} could be adjusted by rising or dropping the control rods in the stationary reflector.

Theoretical Estimation Formula

Pulse parameters under stable operation, including relative power $P_{\max}/P_{\mathrm{t}}$ and relative energy $E_{\mathrm{b}}/E_{\mathrm{t}}$, are critically important in measuring the dynamic performance of the fast periodic pulsed reactor. In order to study $P_{\max}/P_{\mathrm{t}}$ and $E_{\mathrm{b}}/E_{\mathrm{t}}$ in detail and to show the difference between IBR-2 and FPPRU1 dynamics intuitively, the theoretical estimation formulas are derived in the article.

From **Eq. 2**, the following could be obtained:

$$\int_0^T \sum_{i=1}^{6} \frac{\mathrm{d}C_i(t)}{\mathrm{d}t}\mathrm{d}t = \int_0^T \sum_{i=1}^{6} \alpha_i \frac{\beta_{\mathrm{eff}}}{\Lambda} P(t)\mathrm{d}t - \int_0^T \sum_{i=1}^{6} \lambda_i C_i(t)\mathrm{d}t. \tag{4}$$

When the reactor is under stable periodic pulse operation, the production and the decay of delayed neutron precursors reach a balance; as a result, $C_i(0) \approx C_i(T)$ and $\int_0^T \sum_{i=1}^{6} \frac{\mathrm{d}C_i(t)}{\mathrm{d}t}\mathrm{d}t \approx 0$. As the peroid T is about several milliseconds, the variation of the delayed neutron precursors concentration in one period is very small, and $\sum_{i=1}^{6} \lambda_i C_i(t) \approx S$ (S is a constant) is reasonable. Then the following could be obtained:

$$E_{\mathrm{t}} = \frac{\Lambda T}{\beta_{\mathrm{eff}}} S. \tag{5}$$

As shown in **Figure 5**, from time t_{b}, the core reactivity stabilizes at ρ_{b} and the following is obtained:

$$\frac{\mathrm{d}P(t)}{\mathrm{d}t} = \frac{\rho_{\mathrm{b}} - \beta_{\mathrm{eff}}}{\Lambda} P(t) + \sum_{i=1}^{6} \lambda_i C_i. \tag{6}$$

Integrating **Eq. 6** on both side from t_{b} to T, the following is obtained:

$$\int_{t_{\mathrm{b}}}^{T} \frac{\mathrm{d}P(t)}{\mathrm{d}t}\mathrm{d}t = \int_{t_{\mathrm{b}}}^{T} \frac{\rho_{\mathrm{b}} - \beta_{\mathrm{eff}}}{\Lambda} P(t)\mathrm{d}t + \int_{t_{\mathrm{b}}}^{T} \sum_{i=1}^{6} \lambda_i C_i \mathrm{d}t. \tag{7}$$

From time t_{b}, the power decreases at the decay rate of the delayed neutron precursors, as shown in **Figure 5**. As the change of power within time $t_{\mathrm{b}} \sim T$ is very little, the left-hand term of **Eq. 7** is approximately 0. Then it could be achieved as follows:

$$E_{\mathrm{b}} = \frac{S\Lambda}{\beta_{\mathrm{eff}} - \rho_{\mathrm{b}}} (T - t_{\mathrm{b}}). \tag{8}$$

From **Eqs. 5**, **7**, $E_{\mathrm{b}}/E_{\mathrm{t}}$ takes the form as follows:

$$\frac{E_{\mathrm{b}}}{E_{\mathrm{t}}} = \frac{\beta_{\mathrm{eff}}}{\beta_{\mathrm{eff}} - \rho_{\mathrm{b}}} \frac{T - t_{\mathrm{b}}}{T}. \tag{9}$$

Assuming the integral pulse energy Ep is proportional to the product of peak power $P_{\max}$ and half-width t_{h}, then the following can be obtained:

$$E_{\mathrm{P}} = kP_{\max}t_{\mathrm{h}}. \tag{10}$$

k in **Eq. 10** is the proportional coefficient. For IBR-2 with PuO_2 as fuel, according to the experimental data, $k \approx 1$. For FPPRU1,

TABLE 4 | Comparison of FPPRU1 pulse parameters with IBR-2 pulse parameters.

Parameters	IBR-2			FPPRU1	
	Critical search method	Theoretical estimation formula	Experimental data	Critical search method	Theoretical estimation formula
E_b/E_t	6.61%	6.50%	~7% Bondarchenko et al. (2001)	27.74%	28.05%
P_{max}/P_t	687.73	763.30	~750 Dragunov et al. (2012)	185.46	183.25
t_h/μs	236.50	—	245 Pepelyshev and Popov (2006a)	790.95	—
$\rho_{max}/10^{-5}$	301.97	—	304.5–306 Pepelyshev and Popov (2006a)	523.5	—

according to the numerical results of the critical search method, $k \approx 1.5$. Using **Eqs. 9**, **10**, the following could be obtained:

$$\frac{P_{max}}{P_t} = \frac{E_p/(kt_h)}{E_t/T} = \frac{T}{kt_h}\left(1 - \frac{\beta_{eff}}{\beta_{eff} - \rho_b}\frac{T - t_b}{T}\right). \quad (11)$$

Eqs. 9, **11** are the theoretical estimation formula describing E_b/E_t and P_{max}/P_t respectively. As can be seen intuitively from **Eqs. 9**, **11**, P_{max}/P_t increases with the rise of $|\rho_b|$ and T, and with the drop of β_{eff} and t_h. E_b/E_t decreases with the rise of $|\rho_b|$ and the drop of β_{eff}. Thus, the theoretical estimation formula provides a simple way to analyze the factors affecting the pulse parameters clearly and intuitively, and establish a theoretical basis for improving the quality of the pulse parameters.

Comparison of Pulse Parameters of IBR-2 and FPPRU1

The qualities of pulse parameters of the fast periodic pulsed reactors with different fissile materials as fuel are quite different. In this article, the pulse parameters of IBR-2 with PuO_2 as fuel are compared with those of FPPRU1 with UO_2 as fuel. The results are shown in **Table 4**.

As shown in **Table 4**, both the critical search method and the theoretical estimation formula are used to calculate the pulse parameters. For IBR-2, the results obtained with the critical search method are in good agreement with the experimental data on the whole. E_b/E_t calculated with the two methods is in good accordance, proving both the two methods are feasible. It should be noted that P_{max}/P_t obtained with the theoretical estimation formula is on the assumption that k is known in the calculation ($k = 1$ for IBR-2 and $k = 1.5$ for FPPRU1).

It could be known from **Table 4** that, the relative peak power P_{max}/P_t of FPPRU1 is much lower and the relative background energy E_b/E_t is much higher. Thus, the quality of pulse parameters of FPPRU1 is worse than that of IBR-2. From **Eq. 9**, it is known that if β_{eff} is larger, then E_b/E_t is larger and P_{max}/P_t is smaller, which means the quality of pulse parameters is worse. The number of the delayed neutron produced by U-235 and Pu-239 per fission are 0.0068 and 0.00215 (Huang, 2007), respectively. And β_{eff} of FPPRU1 and IBR-2 are 0.00728 and 0.00216, respectively. Thus, the pulse parameters of FPPRU1 are of relative poor quality compared to that of IBR-2.

From **Eqs. 9**, **11**, we know that some measures could be taken to increase the quality of pulse parameters of FPPRU1. For example, the period T could be increased by reducing the rotating speed of moving reflectors. And the half-width t_h could be decreased by optimizing the reactor design. However, the measures may conflict with each other. For instance, reducing the rotation speed of the moving reflectors would also increase the half-width t_h at the same time.

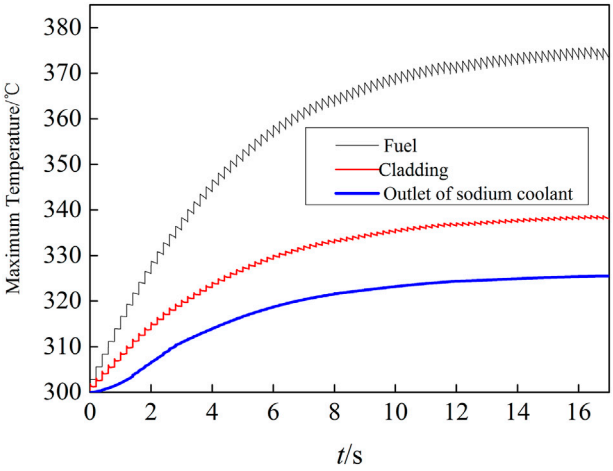

FIGURE 10 | The sub-channel model of the fuel assembly.

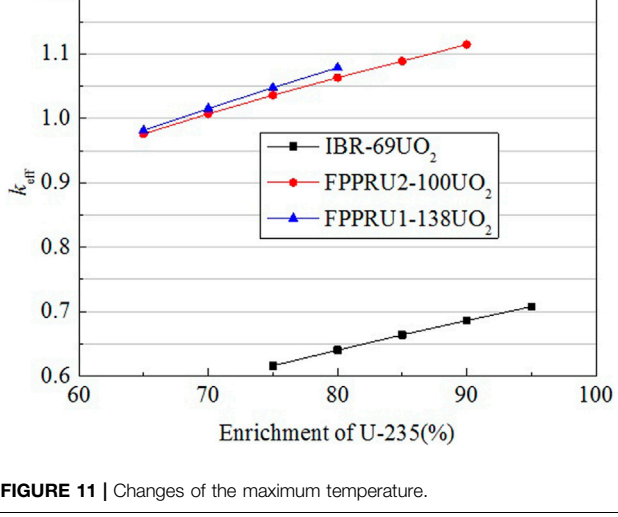

FIGURE 11 | Changes of the maximum temperature.

Thermal Hydraulics Calculation

When FPPRU1 is under stable periodic operation at the average power 2MW, the peak power is about 370.92 MW. For the fuel assembly with the maximum power, the energy deposition in one pulse is about 4 kJ. The pulse frequency is 5 Hz and the half-width is 523.5 μs. The sub-channel model of the fuel assembly with the maximum power for analyzing the thermal hydraulic characteristics is established with FLUENT, as shown in **Figure 10**.

The model in **Figure 10** is 1/12 of the whole fuel assembly shown in **Figure 4**. In the calculation, it is assumed that the inlet temperature of the sodium coolant is 300 ˚C and the flow rate of sodium coolant in one fuel assembly is 800 L/h. The changes of the maximum temperature of the fuel and the cladding and the maximum outlet temperature of sodium coolant are shown in **Figure 11**.

As seen from **Figure 11**, the temperature of the fuel and the coolant rise gradually and reach the balance after operating for about 17 s. The pulses only cause small jagged fluctuations to the temperature. The maximum fuel temperature and the coolant outlet temperature are 375 and 325 ˚C respectively, which means that the thermal safety under stable periodic operation could be guaranteed.

DISCUSSION

The sodium cooling fast periodic pulsed reactor with UO_2 as fuel (FPPRU) is designed, and the feasibility is studied in this article. Two typical core load schemes (FPPRU1 and FPPRU2) with stainless steel or beryllium as the reflector are compared. It is found that FPPRU1 with the stainless steel as the reflector has better performance such as narrower half-width of the pulse, harder neutron energy spectrum on the reflector surface, and less energy deposition in the stationary reflector. On the other hand, the downside of FPPRU1 is that more fuel assemblies have to be loaded to reach criticality. In order to study the reactor dynamics, the critical search method is established. Furthermore, the theoretical estimation formula which could clearly show the difference between the pulse parameters of FPPRU1 and IBR-2 is derived. The two methods are verified by the IBR-2 experimental data and are applied to the calculation of FPPRU1. The results show that the quality of the pulse parameters of FPPRU1 is not as good as that of IBR-2. In order to study the thermal safety under stable periodic operation, the sub-channel model of the FPPRU1 fuel assembly is built, and it is found that the maximum fuel temperature is not very high and thus is acceptable. On the whole, the sodium cooling fast periodic pulsed reactor with UO_2 as fuel is feasible in neutronics and thermal hydraulics, but the quality of the pulse parameters needs to be improved further.

DATA AVAILABILITY STATEMENT

The original contributions presented in the study are included in the article/Supplementary Material; further inquiries can be directed to the corresponding author.

AUTHOR CONTRIBUTIONS

All authors listed have made a substantial, direct, and intellectual contribution to the work and approved it for publication.

REFERENCES

Ananiev, V. D., Lukasevich, I. B., Popov, V. E., and Romanova, N. V. (2020). IBR-2 Run Optimization Suggestions. *At. Energ.* 127 (3), 131–133. doi:10.1007/s10512-020-00598-3

Ananiev, V. D., Pepelyshev, Y. N., and Rogov, A. D. (2019). Optimization Study of the IBR-2 Reactor. *Phys. Atom. Nuclei* 82 (8), 1162–1174. doi:10.1134/S1063778819080039

Ata-Allah, S. S., Balagurov, A. M., Hashhash, A., Bobrikov, I. A., and Hamdy, S. (2016). Refinement of Atomic and Magnetic Structures Using Neutron Diffraction for Synthesized Bulk and Nano-Nickel Zinc Gallate Ferrite. *Physica B: Condensed Matter* 481 (481), 118–123. doi:10.1016/j.physb.2015.10.030

Avdeev, M. V., Rulev, A. A., Ushakova, E. E., Kosiachkin, Y. N., Petrenko, V. I., Gapon, I. V., et al. (2019). On Nanoscale Structure of Planar Electrochemical Interfaces Metal/liquid Lithium Ion Electrolyte by Neutron Reflectometry. *Appl. Surf. Sci.* 486, 287–291. doi:10.1016/j.physb.2015.10.03010.1016/j.apsusc.2019.04.241

Badawy, W. M., Duliu, O. G., Frontasyeva, M. V., El-Samman, H., and Mamikhin, S. V. (2020). Dataset of Elemental Compositions and Pollution Indices of Soil and Sediments: Nile River and delta -Egypt. *Data in Brief* 28 (105009), 105009–105010. doi:10.1016/j.dib.2019.105009

Bondarchenko, E. A., Pepyolyshev, Y. N., and Popov, A. K. (2001). Influence of Automatic Regulator Parameters on Power Transition Processes of the IBR-2 Reactor. *Ann. Nucl. Energ.* 28, 63–78. doi:10.1016/j.anucene.2006.04.002

Brezhnev, A. I., Gulevich, A. V., Kukharchuk, O. F., and Fokina, O. G. (2017). Assessment of the Critical Condition for the Operation of an IBR Reactor with a Subcritical Unit in an Equilibrium Mode. *Nucl. Energ. Tech.* 3 (2), 127–132. doi:10.1016/j.nucet.2017.05.007

Chan, L. Y., and Pepelyshev, Y. N. (2010). IBR-2 Dynamics with Power Shedding. *At. Energ.* 109 (2), 75–80. doi:10.1007/s10512-010-9326-8

Chan, L. Y., and Pepelyshev, Y. N. (2008). Model of IBR-2 Power Feedback Dynamics Taking Account of Slow Components. *At Energy* 104 (4), 262–267. doi:10.1007/s10512-008-9026-9

Dragunov, Y. G., Tretiyakov, I. T., Lopatkin, A. V., Romanova, N. V., Lukasevich, I. B., Ananyev, V. D., et al. (2012). Modernization of the IBR-2 Pulsed Research Reactor. *At Energy* 113 (1), 29–38. doi:10.1007/s10512-012-9591-9

Golovin, I. S., Mohamed, A. K., Bobrikov, I. A., and Balagurov, A. M. (2020). Time-Temperature-Transformation from Metastable to Equilibrium Structure in Fe-Ga. *Mater. Lett.* 263 (127257), 127257–127264. doi:10.1016/j.matlet.2019.127257

Huang, Z. Q. (2007). *Basis of Nuclear Reactor Dynamics*. Beijing, China: Peking University Press.

Kulikov, S. A., and Shabalin, E. P. (2013). Optimization of IBR-2M Moderator Parameters. *At Energy* 115 (1), 48–52. doi:10.1007/s10512-013-9747-2

Marina, F. (2011). Neutron Activation Analysis in the Life Sciences. *Phys. Particles Nuclei* 42 (2), 332–378. doi:10.1134/S1063779611020043

Pepelyshev, Y. N., and Popov, A. K. (2006). Influence of the Nearest Environment of the Core on the Power Pulse Dynamics in the IBR-2 Reactor. *Ann. Nucl. Energ.* 33, 813–819. doi:10.1016/j.anucene.2006.04.002

Pepelyshev, Y. N., and Popov, A. K. (2006). Investigation of Dynamical Reactivity Effects of IBR-2 Moving Reflectors. *At Energy* 101 (2), 549–554. doi:10.1007/s10512-006-0129-x

Pepelyshev, Y. N., Popov, A. K., and Sumkhuu, D. (2017). IBR-2M Reactor Power Feedback Parameters Evaluation Using Square Reactivity Oscillations. *At Energy* 122 (5), 75–80. doi:10.1007/s10512-017-0238-8

Pepelyshev, Y. N., Popov, A. K., and Sumkhuu, D. (2015). Model of the IBR-2M Pulsed Reactor Dynamics for Investigating Transition Processes in a Wide

Range of Power Variation. *Ann. Nucl. Energ.* (85), 488–493. doi:10.1016/j.anucene.2015.06.002

Pepelyshev, Y. N., Vinogradov, A. V., and Rogov, A. D. (2010). "On Some Issues of Safety of Research Pulsed Reactor IBR-2," in International Conference on Current Problems in Nuclear Physics and Atomic Energy, Kiev (Ukraine), June 7–12.

Turchenko, V., Kostishyn, V. G., Trukhanov, S., Damay, F., Porcher, F., Balasoiu, M., et al. (2020). Crystal and Magnetic Structures, Magnetic and Ferroelectric Properties of Strontium Ferrite Partially Substituted with in Ions. *J. Alloys Compounds* 821 (153412), 153412–153417. doi:10.1016/j.jallcom.2019.153412

Conflict of Interest: The authors declare that the research was conducted in the absence of any commercial or financial relationships that could be construed as a potential conflict of interest.

Publisher's Note: All claims expressed in this article are solely those of the authors and do not necessarily represent those of their affiliated organizations, or those of the publisher, the editors and the reviewers. Any product that may be evaluated in this article, or claim that may be made by its manufacturer, is not guaranteed or endorsed by the publisher.